Demonstration of Temporal Distinguishability in a Four-Photon State and a Six-Photon State

G. Y. Xiang,[1] Y. F. Huang,[1] F. W. Sun,[1] P. Zhang,[1] Z. Y. Ou,[1,2,*] and G. C. Guo[1]

[1]*Key Laboratory of Quantum Information, University of Science and Technology of China, CAS, Hefei, 230026, People's Republic of China*

[2]*Department of Physics, Indiana University–Purdue University Indianapolis, 402 North Blackford Street, Indianapolis, Indiana 46202, USA*

(Received 30 January 2006; published 14 July 2006)

An experiment is performed to demonstrate the temporal distinguishability of a four-photon state and a six-photon state, both from parametric down-conversion. The experiment is based on a multiphoton interference scheme in a recently discovered projection measurement of a maximally entangled N-photon state. By measuring the visibility of the interference dip, we can distinguish the various scenarios in the temporal distribution of the pairs and, thus, quantitatively determine the degree of temporal distinguishability of a multiphoton state.

DOI: 10.1103/PhysRevLett.97.023604 PACS numbers: 42.50.Dv, 03.67.Mn, 42.50.St

It is been well known by now that multiparticle entanglement provides more dramatic violations of local realism by quantum theory [1]. It was shown that the number of violations increases with the number of particles [2]. Experimental demonstrations of violations of local realism have thus been shifted from the traditional test of two-photon Bell's inequalities [3–5] to the test of generalized Bell's inequalities for three or four photons in various states [6–10]. While entangled two-photon states are produced naturally from parametric down-conversion, generation of three- and four-photon entangled states has to rely on simultaneous two-pair production in parametric down-conversion. Since pairs are produced randomly in the parametric down-conversion process, this raises a question: Are the two pairs really in an entangled four-photon state or they are simply independent uncorrelated two pairs?

This question was first attempted by Ou, Rhee, and Wang [11,12] in an experiment similar to the famous Hong-Ou-Mandel experiment [13] but with two pairs of photons. Recently, a number of experiments were performed to further address the problem of photon pair distinguishability in parametric down-conversion [14–17]. All the experimental schemes are more or less some sort of multiphoton interference (either two-photon or four-photon). More recently, a new scheme was proposed by Ou [18] that relies on a newly discovered projection measurement process of a maximally entangled N-photon state (NOON state) [19–21] to characterize quantitatively the degree of temporal distinguishability of an N-photon state. When it applies to photon pairs from parametric down-conversion, it shows various visibility of multiphoton interference for different scenarios in the temporal distributions of the photons [18].

In this Letter, we wish to report on an experimental implementation of the NOON-state projection measurement for characterizing the temporal distinguishability of photon pairs from parametric down-conversion. We find that the temporal distinguishability depends on the visibility of multiphoton interference in a NOON-state projection. When the pairs are indistinguishable from each other, we obtain the maximum visibility close to 1. But when the pairs are separated from each other, the visibility drops from one to some nonzero values depending on the scenarios of pair separation.

The key idea in Ref. [18] for characterizing temporal distinguishability is the NOON-state projection measurement, as depicted in Fig. 1 for $N = 4$ and 6. This was recently proposed and demonstrated by Sun *et al.* [19,21] and Resch *et al.* [20] for a multiphoton de Broglie wavelength. This measurement projects an arbitrary two-mode N-photon state of polarization in the form of

$$|\Psi_N\rangle = \sum_k c_k |N-k\rangle_H |k\rangle_V, \tag{1}$$

to a NOON state defined as $|\mathrm{NOON}\rangle \equiv (|N\rangle_H|0\rangle_V - |0\rangle_H|N\rangle_V)/\sqrt{2}$. As a result, an N-photon detection probability is measured that is proportional to

$$P_N \propto |\langle \mathrm{NOON}|\Psi_N\rangle|^2. \tag{2}$$

The physics behind this projection measurement is an ingenious arrangement [22,23] of beam splitters, phase shifters, and projection polarizers for the cancellation by destructive interference of the middle terms in the form of

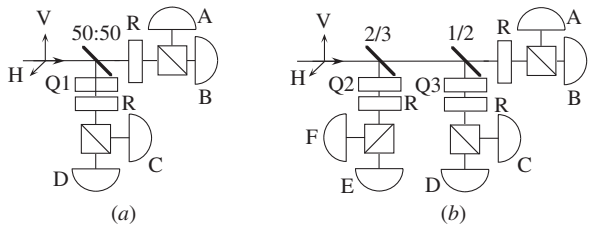

FIG. 1. A NOON-state projection measurement for (a) four photons and (b) six photons. Q1, Q2, and Q3 are wave plates that introduce a relative phase shift of $\pi/2$, $2\pi/3$, and $4\pi/3$, respectively, between H and V. R is a rotator of 45°.

$|N-k\rangle_H|k\rangle_V$, with $k \neq 0$, N in Eq. (1). In particular, for $|\Psi_4\rangle = |2\rangle_H|2\rangle_V$ and $|\Psi_6\rangle = |3\rangle_H|3\rangle_V$, the projection probability in Eq. (2) is zero due to orthogonality. These two states are readily available from type-II parametric down-conversion (PDC) with a quantum state of

$$|\mathrm{PDC}\rangle = |0\rangle + \eta|1\rangle_H|1\rangle_V + \sqrt{2}\eta^2|2\rangle_H|2\rangle_V + \sqrt{6}\eta^3|3\rangle_H|3\rangle_V + \ldots, \quad (3)$$

where $|\eta|^2 \ll 1$ is the pair production probability.

However, the expression in Eq. (2) is for a single mode treatment, which means that the four photons or six photons must be in a single temporal mode (the so-called 4×1 or 6×1 case). So the pairs must be indistinguishable in the production process. This is normally achieved with an ultrashort pump pulse for parametric down-conversion so that the time of the pair production is restricted in the time duration defined by the pump pulse. But because of the finite duration of the pump pulse, this is only approximately the case in practice. So the pairs actually have partial indistinguishability, and this will be reflected in the reduced visibility in the multiphoton interference in the NOON-state projection measurement. As suggested in Ref. [18], the visibility is then a direct measure for the degree of indistinguishability.

The experimental arrangement is shown in Fig. 2. A 2-mm long β-barium borate (BBO) crystal cut for type-II parametric down-conversion is pumped at 390 nm by a frequency-doubled Ti:sapphire pulse laser. The pump pulse has a width of 150 fsec and a repetition rate of $R_0 =$ 76 MHz. The crystal is so oriented that the two conic down-converted fields (o and e rays) at the degenerate frequency converge into two unidirectional beams [24]. The two fields are then coupled to single mode polarization preserving optical fibers. The outputs of the fibers are directed to a polarization beam splitter (PBS) to merge into one beam. One of the fiber outputs is mounted on a translational stage so that we can adjust the relative delay $c\Delta T$ between the two polarizations. The recombined beam, after passing through an interference filter of 3 nm width, is sent to the corresponding NOON-state projection measurement assembly for either the four- or the six-photon case depicted in Fig. 1. All combinations of two-photon (say, AB, AC, etc.) and four-photon coincidence (say, $ABCD$, $ACBE$, etc.) as well as six-photon coincidence ($ABCDEF$) in the six-photon case are measured as a function of the relative delay $c\Delta T$ between the two polarizations. Because of the vast amount of coincidence data and the lack of coincidence units, we measure each coincidence individually.

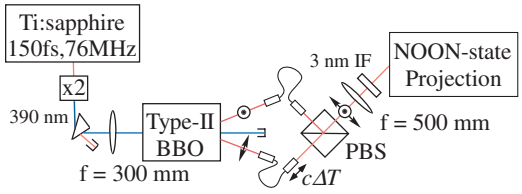

FIG. 2 (color online). Sketch of the experimental setup. IF: interference filter. PBS: polarization beam splitter.

Four-photon case.—When four-photon coincidence is measured in the four-photon NOON-state projection scheme in Fig. 1(a), only the four-photon term in Eq. (3) makes a significant contribution whereas the six-photon term is a higher order (it does produce a background that must be subtracted in data analysis). The four-photon term is from two-pair production. In parametric down-conversion, the two photons within a pair are correlated in time. But for two pairs, there are two extreme cases: (i) The two pairs are generated in the same time and become indistinguishable four photons as in Eq. (3), and we dub it the 4×1 case; (ii) the two pairs are generated at two well separated times and are independent of each other, and we dub it the 2×2 case. In our experiment, case (i) is achieved by the instantaneous pumping from ultrashort pump pulses, while case (ii) is studied from accidental two-pair coincidences (see below).

For the four-photon scheme in Fig. 1(a), there are six possible combinations of two-photon coincidence. They are simply AB, CD, AC, BD, AD, and BC. Among them, AB and CD show the typical two-photon Hong-Ou-Mandel dips [13], with AB shown in Fig. 3(a), whereas the rest is flat (not shown). The visibility of the dip is 89%. The directly measured four-photon coincidence $ABCD$ data after background subtraction are shown as solid circles

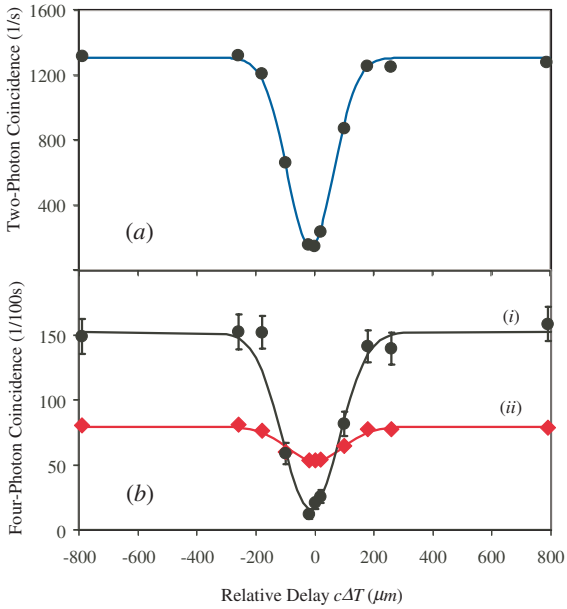

FIG. 3 (color online). (a) Two-photon coincidences and (b) four-photon coincidences as a function of relative delay $c\Delta T$. The circles in (b) are the directly measured $ABCD$ coincidences, while the diamonds are the four-photon coincidences from Eq. (4) corresponding to the 2×2 case. The solid curves are a Gaussian fit with a visibility of 90% and 33%, respectively.

(i) in Fig. 3(b) with a Gaussian fit that has a visibility of 90%. The points in diamonds (ii) are the four-photon coincidences corresponding to the 2×2 case. Since the pairs are independent, the four-photon coincidence are from pairwise accidental coincidence: There are three possibilities of $AB + CD$, $AC + BD$, and $AD + BC$. So the four-photon coincidence in the 2×2 case can be deduced from the measured two-photon coincidences as

$$R_4(ABCD)(2 \times 2) = [R_2(AB)R_2(CD) + R_2(AC)R_2(BD) + R_2(AD)R_2(BC)]/R_0. \quad (4)$$

The solid curve is a Gaussian with a visibility of 33%. All the curves have a width of about 200 μm corresponding to the coherence length from the 3 nm interference filter.

The less than 100% visibility (90%) for the directly measured four-photon coincidence has two origins. One is from an imperfect spatial mode match due to misalignment. This has already reduced the two-photon visibility to 89% in Fig. 3(a). The other origin is from nonoverlapping between the two detected pairs of photons. In other words, the two pairs are not completely indistinguishable for us to treat them as in a single temporal mode and to use Eq. (2) for four-photon coincidence. Reference [19] has a complete account of these two effects and derived the visibility under these imperfect conditions as

$$\mathcal{V}_4 = \frac{2v_2(\mathcal{A} + 3\mathcal{E}) - v_2^2(\mathcal{A} + \mathcal{E})}{3(\mathcal{A} + \mathcal{E})}. \quad (5)$$

Here v_2 is the two-photon visibility from Fig. 3(a). $\mathcal{A}$ is proportional to the absolute square of the four-photon wave function, whereas $\mathcal{E}(\leq \mathcal{A})$ depends on photon pair exchange symmetry. When $\mathcal{E} = \mathcal{A}$, this is the situation when the two pairs of photons are indistinguishable (the 4×1 case). But when $\mathcal{E} = 0$, the two pairs are completely separated from each other and become independent (the 2×2 case) with a four-photon visibility of $\mathcal{V}_4(2 \times 2) = 0.33$ from Eq. (5). This value is exactly the value from curve (ii) in Fig. 3(b). The direct observed four-photon dip in curve (i) in Fig. 3(b) is somewhere in between the two extreme cases. Substituting the observed values of $\mathcal{V}_4 = 0.90$ and $v_2 = 0.89$ in Eq. (5), we obtain $\mathcal{E}/\mathcal{A} = 0.90$. The quantity $\mathcal{E}/\mathcal{A}$ thus provides a measure of partial indistinguishability between the pairs. The nonzero value of 0.33 for $\mathcal{V}_4(2 \times 2)$ can be thought of as a result of the indistinguishability between the two photons within each pair. So the directly measured four-photon dip visibility $\mathcal{V}_4$ is a measure of indistinguishability for all the four photons, as suggested in Ref. [18].

$\mathcal{E}/\mathcal{A}$ can be independently measured from two-photon coincidence on one (o or e ray) of the two down-converted fields [11,12]. This is achieved by blocking one of the two beams that come to the PBS. The directly measured value is $\mathcal{E}/\mathcal{A} = 0.77 \pm 0.06$. Another independent method to measure $\mathcal{E}/\mathcal{A}$ is from the ratio of the values at infinity delay ($|c\Delta T| = \infty$) in the two data sets in Fig. 3(b). Reference [19] gives the ratio as $1 + \mathcal{E}/\mathcal{A}$, and, from Fig. 3(b), we find $\mathcal{E}/\mathcal{A} = 0.92$. This value is more consistent with the one derived from visibility than the value from two-photon coincidence measurement. We believe that this is caused by a spatial mode mismatch between the two pairs of photons [21]. The four-photon coincidence is more restricted than two-photon coincidence and thus acts as some sort of spatial mode filtering, resulting in a better mode match and higher $\mathcal{E}/\mathcal{A}$ values.

Six-photon case.—With a six-photon coincidence, the terms with less than six photons in Eq. (3) have no contribution. Since the six photons are from three pairs of down-converted photons, there are three extreme cases: (i) The three pairs are generated in the same time and are indistinguishable in the quantum state of $|3\rangle_H|3\rangle_V$ (the 6×1 case); (ii) two of them are indistinguishable but well

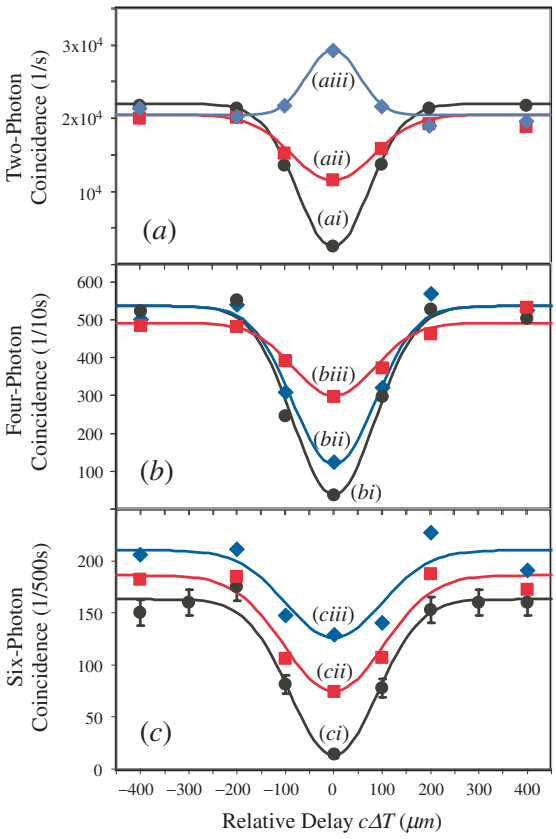

FIG. 4 (color online). (a) Two-photon, (b) four-photon, and (c) six-photon coincidences as a function of relative delay $c\Delta T$. (ai) is for AB, (aii) for AE, and (aiii) for BE in (a). (bi) is for $ABCE$, (bii) for $ABCD$, and (biii) for $BCDE$ in (b). The solid circles (ci) in (c) are the directly measured $ABCDEF$ coincidence, while the diamonds (ciii) are from two-photon data by Eqs. (4) and (6) corresponding to the 2×3 case, and the square points (cii) are from both two-photon and four-photon data by Eq. (6) corresponding to the $4 \times 1 + 2$ case. The solid curves in (c) are a Gaussian fit with a visibility of 92%, 59%, and 39%, respectively. The data in (cii) and (ciii) are multiplied by 2 and 8, respectively, to bring them to a similar scale as (ci).

separated from the third pair; they are in the quantum state of $|2\rangle_{H1}|2\rangle_{V1} \otimes |1\rangle_{H2}|1\rangle_{V2}$ (the $4 \times 1 + 2$ case); (iii) all three pairs are well separated from each other and are in $|1\rangle_{H1}|1\rangle_{V1} \otimes |1\rangle_{H2}|1\rangle_{V2} \otimes |1\rangle_{H3}|1\rangle_{V3}$ (the 2×3 case). The three cases give three different results in the six-photon NOON-state measurement [18].

In the scheme for six photons [Fig. 1(b)], there are 15 different combinations of two-photon or four-photon coincidence. Among the two-photon coincidences, AB, CD, and EF are the same and give a typical Hong-Ou-Mandel dip with 100% visibility in the ideal case; AC, AE, BD, BF, CE, and DF show a dip of an ideal 50% visibility; but AD, BC, CF, DE, AF, and BE have a bump of an ideal 50% visibility. Figure 4(a) shows AB, AC, and AD. Among the four-photon coincidences, $ABCE$, $ABDF$, $CDBF$, $CDAE$, $EFBD$, and $EFAC$ show a dip of 100% visibility ideally; $ABCF$, $ABDE$, $CDBE$, $CDAF$, $EFBC$, and $EFAD$ have a dip of $1/3$ visibility ideally; $ABCD$, $ABEF$, and $CDEF$ have a dip of $5/6$ visibility ideally. They are plotted in Fig. 4(b) after background subtraction. The fitted curves give dips with visibility smaller than the ideal ones. The directly measured six-photon coincidence data are presented in Fig. 4(c) as solid circles (ci). The dip in the fitted Gaussian curve has a visibility of 0.92, as compared to the ideal 100%. The diamond points (ciii) and square points (cii) are six-photon coincidences corresponding to the 2×3 and the $4 \times 1 + 2$ case, respectively. They are deduced from

$$R_6 = \sum_P R_2(P) R_4(P)/R_0, \tag{6}$$

where the index P represents the 15 different combinations of $(AB)(CDEF)$. For the $4 \times 1 + 2$ case (square points), the quantities $R_4(CDEF)$, etc., are directly measured four-photon coincidences [shown in Fig. 4(b)], but for the 2×3 case (diamond points), they are derived from two-photon coincidences by using a formula similar to Eq. (4). The diamond points and the square points are fitted to Gaussian functions with a visibility of $\mathcal{V}_6(2 \times 3) = 0.39$ and $\mathcal{V}_6(4 \times 1 + 2) = 0.59$, respectively. The ideal values are $\mathcal{V}_6^{(0)}(2 \times 3) = 0.4$ and $\mathcal{V}_6^{(0)}(4 \times 1 + 2) = 0.6$ [18].

The observed visibilities in both the 6×1 and the $4 \times 1 + 2$ case are close to the ideal values, indicating that the pairs are almost indistinguishable. This is reflected in the large value of the directly measured $\mathcal{E}/\mathcal{A} = 0.91 \pm 0.04$ from two-photon coincidence, and the $\mathcal{E}/\mathcal{A}$ value would be even closer to 1 for six-photon coincidence. Of course, the observed visibility in 2×3 case is always the predicted value because the two photons in each pair are truly indistinguishable and we have a genuine 2×3 case.

In summary, we used the newly discovered NOON-state projection measurement technique to quantitatively characterize the temporal distinguishability of a four- or six-photon state. We find that the visibility of the multiphoton interference can be used to distinguish different scenarios in the temporal distribution of the photons.

This work was funded by National Fundamental Research Program of China (2001CB309300), the Innovation funds from Chinese Academy of Sciences, and the National Natural Science Foundation of China (Grants No. 60121503 and No. 10404027). Z. Y. O. is also supported by the U.S. National Science Foundation under Grants No. 0245421 and No. 0427647.

*Electronic address: zou@iupui.edu

[1] D. M. Greenberger, M. A. Horne, and A. Zeilinger, in *Bell's Theorem, Quantum Theory, and Conceptions of the Universe*, edited by M. Katafos (Kluwer Academic, Dordrecht, The Netherlands, 1989).
[2] N. D. Mermin, Phys. Rev. Lett. **65**, 1838 (1990).
[3] A. Aspect, P. Grangier, and G. Roger, Phys. Rev. Lett. **47**, 460 (1981); **49**, 91 (1982).
[4] Z. Y. Ou and L. Mandel, Phys. Rev. Lett. **61**, 50 (1988).
[5] Y. H. Shih and C. O. Alley, Phys. Rev. Lett. **61**, 2921 (1988).
[6] J.-W. Pan, D. Bouwmeester, M. Daniell, H. Weinfurter, and A. Zeilinger, Nature (London) **403**, 515 (2000).
[7] J. C. Howell, A. Lamas-Linares, and D. Bouwmeester, Phys. Rev. Lett. **88**, 030401 (2002).
[8] M. Eibl *et al.*, Phys. Rev. Lett. **90**, 200403 (2003).
[9] Z. Zhao *et al.*, Phys. Rev. Lett. **91**, 180401 (2003).
[10] P. Walther, M. Aspelmeyer, K. J. Resch, and A. Zeilinger, Phys. Rev. Lett. **95**, 020403 (2005).
[11] Z. Y. Ou, J.-K. Rhee, and L. J. Wang, Phys. Rev. Lett. **83**, 959 (1999).
[12] Z. Y. Ou, J.-K. Rhee, and L. J. Wang, Phys. Rev. A **60**, 593 (1999).
[13] C. K. Hong, Z. Y. Ou, and L. Mandel, Phys. Rev. Lett. **59**, 2044 (1987).
[14] K. Tsujino, H. F. Hofmann, S. Takeuchi, and K. Sasaki, Phys. Rev. Lett. **92**, 153602 (2004).
[15] H. de Riedmatten *et al.*, J. Mod. Opt. **51**, 1637 (2004).
[16] H. S. Eisenberg, J. F. Hodelin, G. Khoury, and D. Bouwmeester, Phys. Rev. Lett. **94**, 090502 (2005).
[17] Z. Y. Ou, Phys. Rev. A **72**, 053814 (2005).
[18] Z. Y. Ou (to be published); quant-ph/0601118.
[19] F. W. Sun, Z. Y. Ou, and G. C. Guo, Phys. Rev. A **73**, 023808 (2006).
[20] K. J. Resch *et al.*, quant-ph/0511214.
[21] F. W. Sun, B. H. Liu, Y. F. Huang, Z. Y. Ou, and G. C. Guo, quant-ph/0512212.
[22] H. F. Hofmann, Phys. Rev. A **70**, 023812 (2004).
[23] M. W. Mitchell, J. S. Lundeen, and A. M. Steinberg, Nature (London) **429**, 161 (2004).
[24] S. Takeuchi, Opt. Lett. **26**, 843 (2001).